THz Spectra and Dynamics of Aqueous Solutions Studied by the Ultrafast Optical Kerr Effect

ARTICLE *in* THE JOURNAL OF PHYSICAL CHEMISTRY B · FEBRUARY 2011

Impact Factor: 3.3 · DOI: 10.1021/jp111764p · Source: PubMed

3 AUTHORS:

Kamila Mazur

14 PUBLICATIONS **162** CITATIONS

SEE PROFILE

Ismael A Heisler

University of East Anglia

48 PUBLICATIONS **539** CITATIONS

SEE PROFILE

Stephen R. Meech

University of East Anglia

154 PUBLICATIONS **3,594** CITATIONS

SEE PROFILE

THE JOURNAL OF PHYSICAL CHEMISTRY B

ARTICLE

pubs.acs.org/JPCB

THz Spectra and Dynamics of Aqueous Solutions Studied by the Ultrafast Optical Kerr Effect

Kamila Mazur, Ismael A. Heisler, and Stephen R. Meech*

School of Chemistry, University of East Anglia, Norwich NR4 7TJ, U.K.

Supporting Information

ABSTRACT: The nature and extent of the effects that hydrophilic and hydrophobic solutes have on the dynamics of water molecules continues to be an area of intense experimental and theoretical investigation. In this work, we use the ultrafast optical Kerr effect to measure the picosecond dynamics and THz Raman spectral densities of a series of aqueous solutions. The solutes studied are the hydrophilic urea and formamide and the hydrophobic trimethylamine *N*-oxide and tetramethylurea. Measurements are made as a function of concentration between <0.1 M and >4 M. At low concentrations (<0.5 M), the THz spectrum resembles that of bulk water, but the picosecond relaxation time, reflecting dynamics in the water H-bonded network, is increased relative to bulk water for all four solutes. The extent to which water relaxation is slowed down depends on the nature of the solute, and is more pronounced for hydrophilic than for hydrophobic solutes. At concentrations above 1 M, a range of solute−solvent and solute−solute interactions gives rise to diverse solute dependent changes in the THz spectral density and to a further slowing down of the picosecond relaxation. The hydrophobic trimethylamine *N*-oxide has remarkably little effect on the spectral density of water, which may indicate solute self-association and the formation of water pools in more concentrated solutions. For hydrophilic urea and formamide, the THz spectral density suggests that water structure is disrupted at concentrations where most water molecules are part of a solvation shell. At such high concentrations, modes associated with the H-bonded solute make a significant contribution to the spectral density at around 100 cm^{-1}. The hydrophobic tetramethylurea solute makes a substantial contribution to the spectral density, complicating the interpretation, but a line shape analysis suggests that it also does not strongly perturb the water structure.

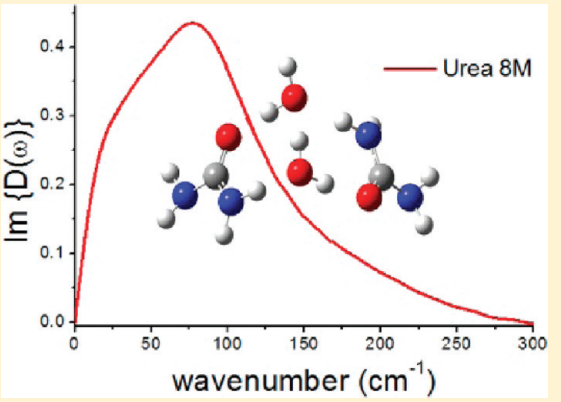

INTRODUCTION

Interfacial water plays a key role in controlling structure, function, and reactivity in biological media and has consequently been the subject of intense research in recent years.[1−13] Differences in the nature of hydration water in the presence of hydrophilic and hydrophobic groups have received particular attention.[1−6,14−16] Hydrophobic and hydrophilic solvation are of critical importance in understanding protein folding and the activity of enzyme proteins.[17] However, the extent to which hydrophilic and hydrophobic groups modify the dynamics of surrounding water molecules remains a matter of discussion. A range of different experimental techniques and molecular dynamics studies have given contradictory results.[7]

To provide a new perspective on this problem, we report here the ultrafast dynamics of aqueous solutions observed through their polarizability anisotropy relaxation, using as solutes prototypical hydrophilic and hydrophobic molecules: trimethylamine *N*-oxide (TMAO), tetramethylurea (TMU), urea (UA), and formamide (FA) (Figure 1). TMAO consists of three hydrophobic methyl groups and a single hydrophilic, negatively charged oxygen. This oxygen contains three lone pairs, and can therefore accept more than two hydrogen bonds.[18] TMU has four methyl groups, while the most hydrophilic part is a single oxygen atom in a carbonyl group. On average, two water molecules can form hydrogen bonds with the carbonyl oxygen.[19] The nitrogen atoms in TMU do not form hydrogen bonds with water in aqueous solutions.[19] Thus, both TMAO and TMU contain mainly hydrophobic groups and act only as hydrogen bond acceptors. UA has two amine groups linked by a carbonyl group, and FA has a single amine group joined to a carbonyl. In both UA and FA, carbonyl and amino groups can form hydrogen bonds, with the former being a hydrogen bond acceptor and the latter a donor. Thus, UA and FA are considerably more hydrophilic than TMAO and TMU.

These solutes have previously been classified as either structure makers or breakers. Typically, the classification is based upon macroscopic observations, such as the sign of the temperature dependence of the *B* coefficient in viscosity measurements.[20] A number of efforts have been made to find a molecular description of this phenomenon. For example, TMAO was reported to be a structure maker, whereas the apparently equally

Received: December 10, 2010
Revised: January 18, 2011
Published: February 28, 2011

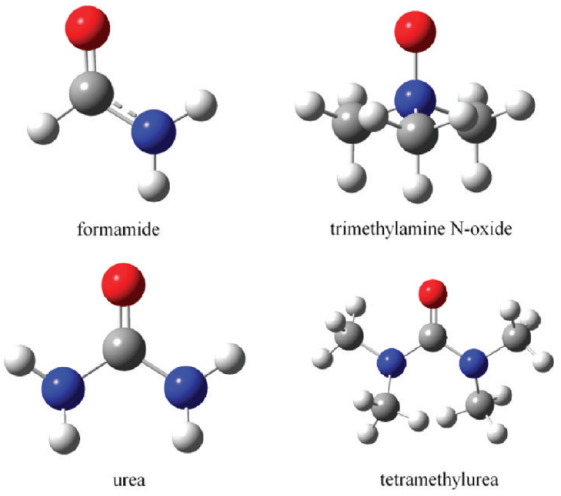

Figure 1. Structure of FA, TMAO, UA, and TMU from DFT calculations.

hydrophobic TMU was classified as a structure breaker on the basis of molecular dynamics simulations.[21] However, Székely et al.[22] using neutron scattering and density measurements reported a structure making capability for TMU. Similarly, there is controversy regarding the effect of UA on the structure of water. From Raman and ultrasonic attenuation measurements,[23,24] it was concluded that UA disrupts the water structure and may therefore be termed a structure breaker. However, dielectric measurements[25] showed that UA is not a strong structure breaker and molecular dynamics simulations classified UA as a structure maker.[26,27] NMR studies of UA solutions have variously reported UA as a structure breaker,[28] or suggested it has little or no effect on water structure.[29] FA has been classified as a structure breaker on the basis of positron annihilation and sound velocity experiments.[30]

In 1945, Frank and Evans[31] reported that the entropy of vaporization of aqueous solutions diverged from that established for nonaqueous solutions. They proposed an "iceberg model" in which water molecules are connected in a quasi-solid-like structure around a hydrophobic solute. Some support for this model was found in the molecular dynamics simulations of Wei et al.[21] who reported that on average individual water−water hydrogen bonds become stronger in the presence of TMU and TMAO molecules. Further, it was found that the TMAO solute led to increased ordering of the water solvent, making it "ice-like" (although no ordering of water molecules was observed upon addition of TMU).[21] Recently, a dynamical rather than structural picture of the "iceberg model" was proposed on the basis of ultrafast time-resolved mid-infrared spectroscopy.[5,6] Much slower orientational dynamics were observed for water in the presence of hydrophobic solutes than was observed for bulk water. From this, it was concluded that each methyl group of TMU and TMAO immobilizes four water OH groups. Hynes and coworkers[14] studied the same systems in aqueous solutions using molecular dynamics simulations and an analytic extended jump model of the orientational dynamics. They found only a moderate slow down of solvent orientational dynamics at low solute concentration (less than a factor of 2 compared to bulk water). The orientational relaxation time was however found to increase with increasing solute concentration. This retardation of water reorientation was explained on the basis of slower H-bond exchange. No convincing evidence for water immobilization was found in these calculations. Hynes and co-workers also reported that hydrophilic groups have a greater impact on water mobility than hydrophobic ones. NMR studies of water dynamics in aqueous solutions of TMAO and TMU suggested that the orientational relaxation time was slowed by the hydrophobic solutes but only by a factor of about 2. It was proposed that the difference between the NMR and transient IR data might arise from the very different concentrations used, those for IR being relatively high, potentially leading to disruption of the water structure.[15]

Water structure around UA has been studied experimentally by IR, neutron, and Raman scattering[2,32,33] and through molecular dynamics simulations.[18,21] No consistent picture regarding the structure and dynamics of water in the presence of UA has emerged.[27,34,35] Idrissi et al.[34] in a molecular dynamics study concluded that water structure was enhanced, and that there is a distortion of the tetrahedral arrangement of water molecules upon addition of UA. In contrast, molecular dynamics simulations by Kuffel et al.[18] found that the geometry of the water−water hydrogen bond network in the solvation layer around UA was essentially the same as that in bulk water. NMR studies of orientational relaxation found that water was largely unaffected by UA.[36] The possibility of self-association of UA molecules with increasing concentration in aqueous solution has been considered. Infrared studies suggested the possibility of the formation of UA dimers, which slightly alter the structure of water,[2] while Monte Carlo simulations suggested that UA dimers are present at ∼1 M concentration, and that above ∼5.5 M a UA network is formed.[3] However, at concentrations below 1 M, UA does not affect the water structure.[3] In contrast to these reports, a neutron scattering study found no evidence for the existence of UA dimers.[33]

In this work, we apply the ultrafast optically heterodyne-detected−optical Kerr effect (OHD−OKE) to investigate the dynamics of aqueous solutions of UA, FA, TMAO, and TMU. The OHD−OKE is a real time technique of sufficient sensitivity to probe changes in solution dynamics at relatively low (<0.1 M) solute concentrations. In addition, it yields both the picosecond relaxation dynamics in the water H-bonded network and the THz Raman spectral density, which contains information on the H-bonding structure in liquid water.[37−39] Thus, the OKE method affords us the unique ability to measure solution dynamics in real time and to correlate them with structural features in the solution, as revealed by the THz spectrum. In addition, the high sensitivity of the method allows the observation of solute effects at lower concentrations than have been accessed in other real time optical experiments; as discussed below, the effect of concentration on the dynamics may resolve some of the key differences between existing measurements in the current literature. In a previous study,[40] we investigated water dynamics in the solvation shell of three amphiphilic dipeptides and found that at low concentration, <0.4 M, the tetrahedral structure of water was largely preserved and the relaxation time slowed down compared to bulk water. Slower dynamics were observed for the more hydrophilic peptide, indicating that hydrophilic sites have a larger effect on the retardation of water dynamics than hydrophobic ones. Here, we apply the same technique to a detailed investigation of the effect of hydrophilic and hydrophobic solutes on the dynamics of water. These data yield new insights into structure and dynamics in aqueous solutions.

EXPERIMENTAL SECTION

The OHD−OKE is a sensitive third order nonlinear optical method which measures the relaxation of induced polarizability anisotropy in real time.[41] The method has been widely applied to study the dynamics of molecular liquids and complex fluids.[42−44] The source used here was a home-built titanium sapphire laser with 300 mW output power and a repetition rate of 68 MHz. The pulses were centered at a wavelength of 810 nm and were of 41 fs duration.

Details of the measurement and analysis procedures can be found elsewhere.[41,45] Briefly, the OHD−OKE is a form of pump−probe polarization spectroscopy. The linearly polarized pump pulse induces a time dependent birefringence in the sample, which is monitored by transmission of the probe pulse, polarized at 45° to the pump, through crossed polarizers. The probe pulse arrives at a pump−probe delay time t set by a variable delay line. The Kerr response $R(t)$, which is measured in a heterodyne detection scheme, contains both an instantaneous electronic hyperpolarizability contribution $\sigma(t)$ and a sum of nuclear contributions $r_i(t)$:

$$R(t) = \sigma(t) + \sum_i r_i(t) \quad (1)$$

The ultrafast pulses are not instantaneous; therefore, the observed signal $S(t)$ is a convolution of the second order autocorrelation of the laser pulses $G_2(t)$ with the molecular nonlinear impulse response $R(t)$:

$$S(\tau) = \int_{-\infty}^{\infty} G_2(t)R(\tau - t)\, dt \quad (2)$$

The signal $S(\tau)$ can generally be separated into subpicosecond and picosecond contributions. The former are typically oscillatory in nature and reflect non-diffusive dynamics and interaction induced effects, while the latter reflect slower intermolecular reorganization and diffusive orientational relaxation.[45]

The subpicosecond response is best treated in the frequency domain, and to focus on these ultrafast dynamics, the picosecond component was fitted with a sum of exponential functions:

$$[1 - \exp(-t/t_r)] \sum_i a_i \exp(-t/\tau_i) \quad (3)$$

and then subtracted from the response.[41] a_i in eq 3 denotes the amplitude and t_r is a rise time, such that eq 3 fulfils the requirements that the signal is zero at $t = 0$; the exact value of the rise time (typically a few tens of femtoseconds) does not influence the results. This separation procedure is somewhat arbitrary but is necessary to permit clear observation of the THz spectrum without a potentially distorting contribution from an intense peak near zero frequency. A comparison of the complete spectral density, with the subtracted spectrum is shown in Figure S3 of the Supporting Information.

The result is the reduced Raman spectral density, $D'(\omega)$, which is calculated from the Fourier transform deconvolution relationship:[46]

$$\frac{\mathrm{FT}[S(\tau)]}{\mathrm{FT}[G_2(\tau)]} = D'(\omega) \quad (4)$$

in which the picosecond response has been subtracted from $S(\tau)$. The imaginary part of the spectral density, Im $D'(\omega)$, reflects only the nuclear part of the Kerr response, independent of pulse width.[46] Im $D'(\omega)$ is directly related to depolarized light scattering (DLS) data,[47] but unlike them, OHD−OKE is undistorted by the thermal population at low frequencies and thus yields the THz Raman spectral density with excellent signal-to-noise.

Samples. FA, TMU, 8 M UA solution, and solid TMAO were purchased from Sigma Aldrich. All samples were used as received, and aqueous solutions were prepared between concentrations of <0.1 M and the maximum possible concentration (4 M saturated solution for TMAO, 8 M UA, neat FA, and neat TMU). In order to reduce light scattering, all samples were filtered through a 0.22 μm Millipore filter. The viscosities for aqueous solutions were taken from the literature.[48−51]

DFT calculations. Ab initio quantum chemistry calculations at the density functional theory level (DFT) were performed in order to assign low frequency Raman modes of the solutes, and to investigate their specific solute−water or solute−solute interactions. The Gaussian 03 program with the B3LYP hybrid functional and the 6-31G (d,p) basis set was used.[52] Optimized molecular structures are given in Figure 1.

RESULTS AND DISCUSSION

Picosecond Molecular Dynamics. *Measurements.* The dynamics of pure water and its THz spectral density have been studied in considerable detail through OHD−OKE and DLS.[38,53−55] Time domain data are shown in blue in Figure 2. The sharp peak at $t = 0$ arises from the instantaneous $\sigma(t)$ response and is followed by the time dependent nuclear component. A complex oscillatory response is apparent in the subpicosecond nuclear dynamics. The Im $D'(\omega)$ (see below and refs 37 and 53) reveals three distinct peaks which are quite characteristic of liquid water. The first is above 400 cm^{-1} and has been assigned to inertial and librational dynamics;[37] this mode is not resolved with the present time resolution. The two lower frequency components at ∼175 and ∼45 cm^{-1} have been assigned to restricted translational modes of water.[56] Specifically, the higher frequency mode was assigned to intermolecular H-bond stretching through MD calculations and by analogy with the spectrum of the tetrahedral structure of ice,[57] while the lower frequency component was assigned to an intermolecular bending mode, although the role of H-bonds in this mode is uncertain.[58−60]

The slower (>1 ps) dynamics of pure water relax monotonically with a non-single-exponential[37] or stretched exponential[38] form. As the polarizability of water is approximately isotropic,[61] molecular orientational relaxation is expected to make a minor (though non-negligible[62]) contribution to this picosecond component (unlike in many other molecular liquids, where diffusive reorientation dominates the slowest relaxation[42,43]). Instead, the relaxation observed in water reflects the picosecond time scale translational and rotational−translational intermolecular dynamics within the H-bonded network.[37,38] In the remainder of this section, we focus on the effect of the four solutes on this picosecond relaxation.

The time domain data for all four aqueous solutions are shown in Figure 2 as a function of concentration. All data were intensity normalized to the electronic response at $t = 0$ ps. FA and UA solutions exhibit qualitatively similar dynamics, with the relaxation time increasing with solute concentration. TMU follows a similar pattern, but the increase associated with the slowest components is much more marked. In contrast, the picosecond dynamics of aqueous TMAO solutions become slower with increasing concentration without a major increase in their amplitude. (Longer time domain data for FA, UA, and TMU solutions

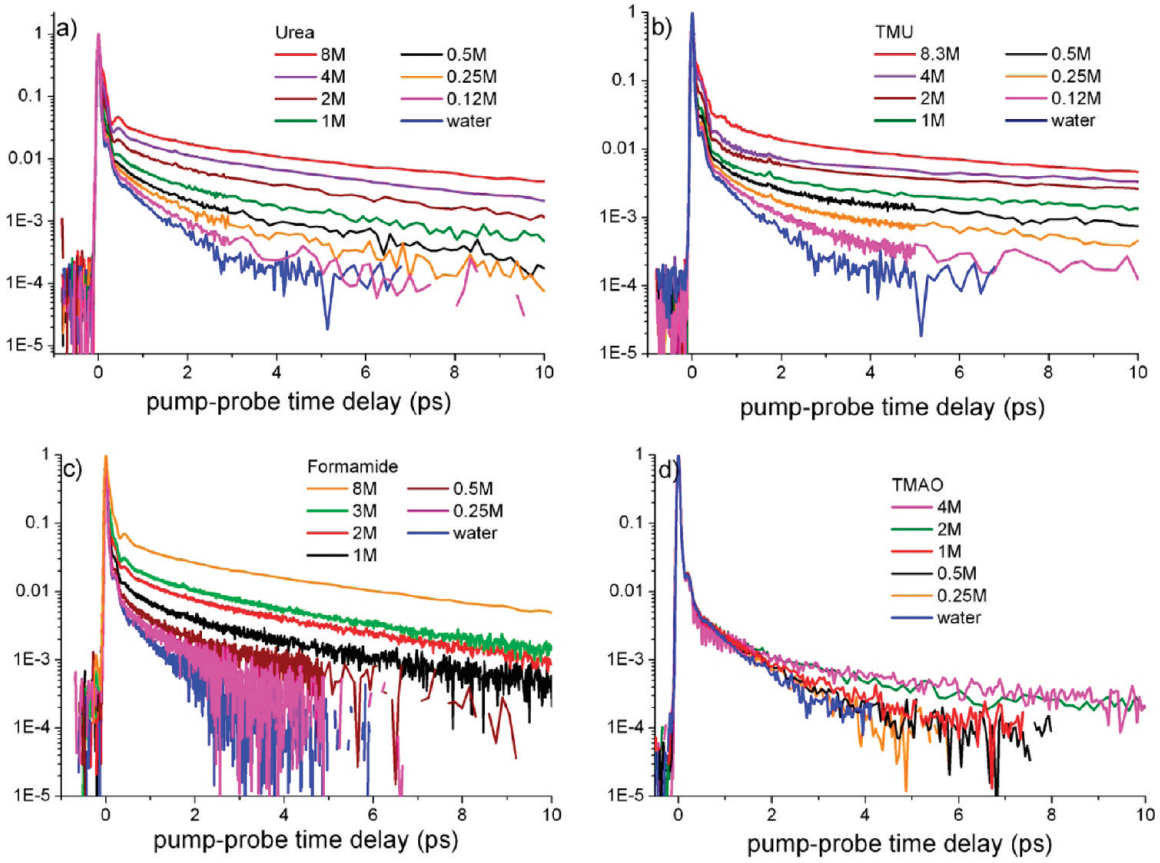

Figure 2. The time-resolved Kerr effect signal of aqueous UA, TMU, FA, and TMAO as a function of concentration, including the bulk water result.

are presented in the Supporting Information.) It is noteworthy that in the high concentration range, associated with increasing amplitude of the slow component, new underdamped (oscillatory) features appear in the subpicosecond response. These features can be seen at around 500 fs for UA and FA solutions and between 200 fs and 1.7 ps for TMAO and TMU solutions (Figure 2). These oscillations are assigned to Raman active solute modes (see below).

The picosecond response was fitted to eq 3. A sum of two exponential relaxation terms was sufficient to reproduce the picosecond dynamics of UA, FA, and TMAO over the entire concentration range. However, a third, longer exponential had to be included to fit the response of TMU. The rise time in eq 3 was kept constant at 100 fs (the picosecond time scale parameters from the fit to eq 3 are insensitive to the exact value of the ultrafast rise time, as previously observed[63]). Data before 1 ps were not included in the fit. Other fitting functions were tried, including the stretched exponential previously employed for peptide solutions.[40] However, the sum of two exponential functions always gave a better fit. It is possible that the distribution of relaxation times is broader for the more complex amphiphilic peptide solutes, thus requiring the use of the stretched exponential function. The amplitudes and relaxation times recovered from the analysis are presented in the Supporting Information.

Data obtained from the fit were used to calculate a weighted mean relaxation time, which is the average relaxation time $\langle\tau\rangle$ according to the equation

$$\langle\tau\rangle = \frac{a_1}{a_1 + a_2}\tau_1 + \frac{a_2}{a_1 + a_2}\tau_2 \qquad (5)$$

In Figure 3, $\langle\tau\rangle$ values for all four solutes are plotted as a function of the molar ratio n_{SW} (where n_{SW} is the ratio of the number of moles of solute to the number of moles of water). The data presented for TMU were obtained from the weighted mean lifetime calculated using the fastest two exponential components only; the long third exponential used in fitting the TMU data is discussed separately below.

Two distinct concentration regions are apparent in Figure 3a. At low concentrations (below $n_{SW} \sim 0.02$), $\langle\tau\rangle$ increases with increasing solute concentration and extrapolates back to the pure water value (Figure 3b). Qualitatively, it is apparent that in this low concentration range the hydrophilic solutes (UA, FA) give rise to a more marked increase in $\langle\tau\rangle$ than the hydrophobic TMAO and TMU. The second region is above $n_{SW} \sim 0.02$ (i.e., >1 M solute concentration), where the slope of $\langle\tau\rangle$ with respect to solute concentration decreases, and the plot no longer extrapolates to the pure water result. In this concentration range, it is possible that in addition to the water relaxation dynamics solute orientational relaxation contributes to the observed OHD−OKE signal, and solute−solute interactions may become significant. These distinct concentration regions are analyzed separately.

Low Solute Concentration. Quantitative analysis (below) will assume that at the lowest concentrations ($n_{SW} < 0.02$) the observed relaxation time is dominated by dynamics in the water H-bonded network. To justify such an assumption, it is necessary to determine the extent to which the solute might contribute to $\langle\tau\rangle$ at these low concentrations. To this end, it was assumed that the relaxation time associated with the solute is given by the longest relaxation time observed at the highest concentration.

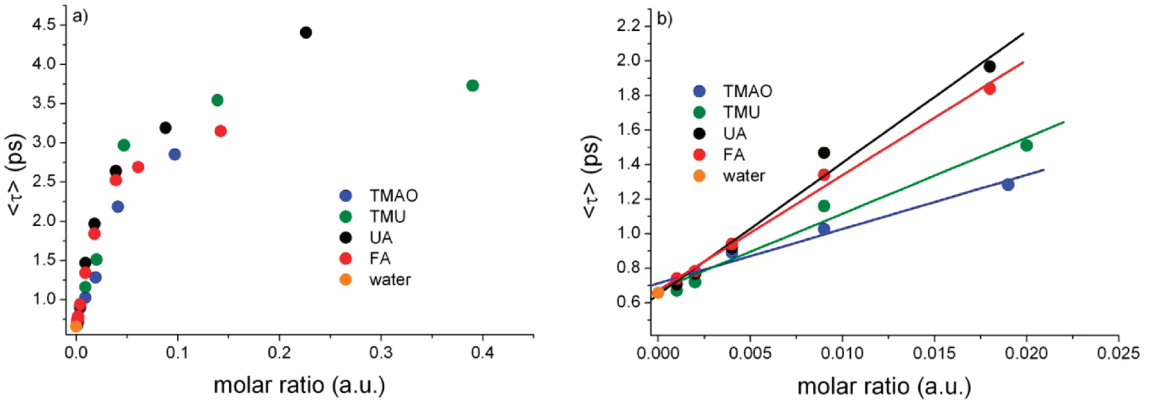

Figure 3. (a) Weighted mean lifetime for TMAO, TMU, UA, and FA plotted as a function of solute solvent molar ratio. (b) Linear fit to the data for molar ratios below 0.02.

From this assumed solute relaxation time, the known relaxation time of pure water and the known mole fractions, a value for $\langle\tau\rangle$ was calculated under the assumption that it is simply a weighted sum of bulk water and solute relaxation times (the latter corrected for viscosity of the solution). The calculated times were invariably smaller than the $\langle\tau\rangle$ obtained from experiment (details of the calculation can be found in the Supporting Information). Thus, we conclude that the slowing down observed in the relaxation at low concentration reflects an effect of the solute on the solvent (water). This assessment of the solute contribution is consistent with the results of MD simulations on FA in water at mole fractions down to 0.05.[64]

To quantitatively model the average effect of the solute on the water dynamics, it is necessary to consider how many water molecules may be affected by a single solute molecule. As a first approximation, we take this to be the number of water molecules in the first solvation shell of each solute, n_m. This was calculated from the relative volumes of water and solute molecules (obtained from DFT calculations); details of the calculation are shown in the Supporting Information. The values are 17, 21, 28, and 32 water molecules for FA, UA, TMAO, and TMU, respectively. These values are in good agreement with previously published data,[15] where hydration numbers were calculated using molecular dynamics simulations. Significantly, at solute concentrations above 1 M, between one-third and all of the water molecules are part of the hydration shell of a solute. Consequently, at these higher concentrations, solvating water molecules are more likely to be H-bonded to each other rather than to a bulk water molecule.

Since OHD−OKE measurements cannot distinguish between hydration water and free water, it is assumed that the relaxation time measured at low n_{SW} is an average of the relaxation times of water molecules in the first solvation shell, τ_{WS}, and bulk (or free) water, τ_{WF} = 0.66 ps,[38,54] weighted by their respective mole fractions, X_i:[65]

$$\langle\tau\rangle = X_{WS}\tau_{WS} + X_{WF}\tau_{WF} \quad (6)$$

For dilute solutions, the above equation can be rewritten as

$$\langle\tau\rangle = n_{SW}n_m(\tau_{WS} - \tau_{WF}) + \tau_{WF} \quad (7)$$

In Figure 3b, linear fits to $\langle\tau\rangle$ data up to n_{SW} = 0.02 are shown. The slope yields $n_m(\tau_{WS}-\tau_{WF})$. Using the calculated n_m, the relaxation times, τ_{WS}, recovered are 1.7 ps for TMAO, 1.9 ps for TMU, 4.2 ps for UA, and 4.4 ps for FA. Thus, water relaxation in the first hydration shell is 2−3 times slower than that in bulk water for the hydrophobic TMAO and TMU solutes and 6−7 times slower for hydrophilic UA and FA. As noted previously,[40] the precise ratio of bulk water to solvating water relaxation times is somewhat dependent on the assumptions made. For example, if the influence of the solute extends beyond the first solvation shell, n_m will be larger and the ratio will thus be smaller (corresponding to a shorter τ_{WS}). Such long-range effects have been suggested in molecular dynamics studies of aqueous carbohydrate solutions.[66] Similarly, if the Raman cross section is enhanced by the interaction between solute and solvent, the ratio will also be decreased.

The magnitude of the slowdown in water dynamics induced by these solutes is similar to that reported in our earlier study of dipeptide solutions.[40] Similar effects have also been observed in DLS studies of glucose−water solutions.[65] Significantly, Figure 3b confirms that the extent of the slowdown depends on the nature of the solute; both hydrophilic and hydrophobic solutes slow down structural relaxation in water, but the effect is significantly larger for the hydrophilic solutes. This is in agreement with our previous measurements of water dynamics around hydrophilic and amphiphilic peptides, and is consistent with the simulations of Laage and Hynes, who reported that hydrophilic solutes have the largest effect on water relaxation dynamics.[16,40] The smaller effect of hydrophobic solutes on water dynamics observed are also consistent with NMR measurements[15] and with a very recent study of dielectric relaxation in *dilute* aqueous TMU.[67] This is significant, as NMR and dielectric relaxation probe mainly orientational relaxation which is not a major contributor to the dynamics observed here; evidently there is a correlation between orientational relaxation and the more collective H-bond network relaxation observed in OKE. In contrast, for the low concentration regime of Figure 3b, we do not find evidence for immobilization of water molecules by hydrophobic solutes, such as has been observed in transient IR studies.[5]

High Solute Concentration. At higher concentrations (above 1 M), almost all water molecules are in the first hydration shell of a solute; therefore, relation 7 does not hold. Under these conditions, the amplitude of the slowest relaxation time increases more rapidly than that of the fastest component (Figure 2) and comes to dominate the relaxation. As a result, the significant changes in amplitudes are not accompanied by large increases in relaxation time; e.g., the change in τ_2 between 1 and 8 M for FA is only a factor of 0.87 (see Table S2 in the Supporting

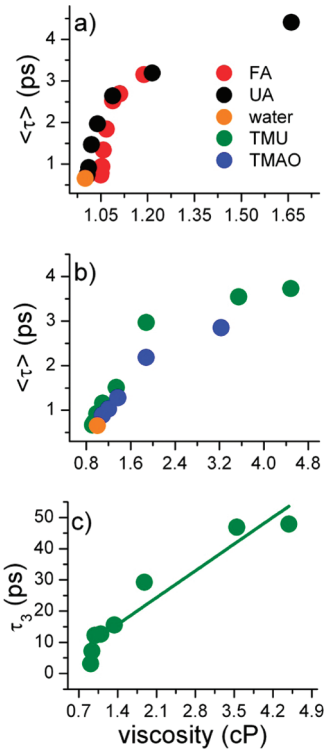

Figure 4. Dependence of $\langle\tau\rangle$ on viscosity for (a) UA and FA and (b) TMAO and TMU. (c) The slowest relaxation time, τ_3, for TMU plotted as a function of viscosity.

Information), which is reflected in the concentration dependent $\langle\tau\rangle$, where relatively small increases are observed for concentrations above 1 M (Figure 3). This suggests a growing contribution from slow structural relaxation in these more concentrated solutions; a similar phenomenon was noted in concentrated aqueous dipeptide solutions.[40] Because almost all water molecules are involved in forming solvation shells, their ability to form the H-bonded tetrahedral structures characteristic of bulk water is limited. This effect is explored further in the study of the THz spectral density, below. The present data are however consistent with the appearance of significantly slower relaxation dynamics at high concentrations, accompanying the formation of an H-bonded solvent−solute network, isolating water molecules from a tetrahedral environment. Quantitative analysis of these data is hampered by the unknown extent to which the solute contributes to the OKE signal at higher concentrations.

Slow orientational dynamics were reported by Rezus et al.[6] in their mid-infrared ultrafast pump−probe studies of vibrational and orientational relaxation of HDO molecules in relatively concentrated (>0.4 M) aqueous solutions of TMU. Reorientation times in excess of 10 ps were observed, which was assigned to approximately 15 OH groups being immobilized by the methyl groups of TMU. This is an appreciably slower relaxation than is observed here for higher concentrations of the hydrophobic solute TMAO (comparison with TMU is more difficult due to a solute contribution to the OKE signal, see below). Bakker and coworkers concluded that the slowdown of the water reorientation in the first solvation shell of the solute originates from steric effects; the solute prevents a fifth water molecule from approaching a tetrahedrally coordinated water molecule, thus preventing molecular reorientation.

Laage at al.[16] extended their simulations of water reorientation near the hydrophobic and hydrophilic parts of TMAO to relatively high concentrations, in excess of 1 M. They found that water molecules reorient only about 1.5 and 4 times more slowly than those in bulk-like water next to hydrophobic and hydrophilic sites, respectively. They suggested that the retardation of water dynamics originates from a combination of two effects. First is that the oxygen in TMAO forms stronger H-bonds with water molecules than are formed between pairs of water molecules. This process is approximately concentration independent. The second is a solute-induced transition state excluded volume fraction effect. The presence of the hydrophobic groups prevents the approach of water H-bond acceptors, thus retarding the jump rate between water molecules around hydrophobic sites. This gives rise to a concentration dependent slowing in the orientational dynamics. These simulations are qualitatively consistent with the data reported above (although OHD−OKE measures structural relaxation in the water network rather than orientational relaxation). Interestingly, Laage and co-workers suggested that the effect of concentration on reorientation might be larger because of the concentration dependent viscosity of the solutions.[14]

In Figure 4, the relationship between the measured relaxation time $\langle\tau\rangle$ and solution viscosity is considered. The changes in viscosity for FA and UA are very small, at most 65% over the full concentration range, while the increase in $\langle\tau\rangle$ is large (a factor of ca. 7 for UA), Figure 4a. The increases in $\langle\tau\rangle$ observed for TMU and TMAO are of a similar order to those for FA and UA, but the viscosity change is much larger (increasing by up to a factor of 5) over the same concentration range, Figure 4b. From these data, we conclude that viscosity has at most a minor effect on the relaxation time observed in OHD−OKE.

TMU was the only solute studied for which three exponential functions were required to fit the picosecond dynamics. The relaxation time (τ_3) obtained from the third exponential is plotted in Figure 4c where it is shown to scale linearly with solution viscosity, consistent with the Stokes−Einstein−Debye (SED) relation, $\tau_3 = V\eta/k_BT$, where V is the hydrodynamic volume and η is the viscosity. This dependence suggests the assignment of τ_3 to orientational relaxation of TMU. The viscosity of TMAO is similar to that of TMU. However, the signal for TMAO at high concentration was several times smaller and it was not possible to resolve a third exponential. This implies that the TMAO solute contributes at most a minor component to the picosecond relaxation dynamics, which thus reflects dynamics in the solvating water molecules, consistent with the preceding analysis.

Raman Spectral Density. The concentration dependent Im $D'(\omega)$ of UA, TMU, FA, and TMAO solutions are shown in Figure 5. All data were normalized in the time domain to the electronic response prior to the Fourier transform. The validity of this normalization procedure was checked by measuring absolute OHD−OKE amplitudes separately at $t = 0$ ps for all samples. Up to 1 M concentration, the absolute amplitudes for all solutions were the same as for pure water within experimental error. Above 1 M, the amplitude increases, reflecting the onset of a measurable solute contribution. The largest increase was observed for TMU. For example, the amplitude at $t = 0$ for 8 M TMU was twice that of 8 M UA, while that for 8 M UA was only a factor of 1.25 greater than that for pure water. UA, TMAO, and FA all had a similar weak dependence of the absolute amplitude on concentration. The relatively large

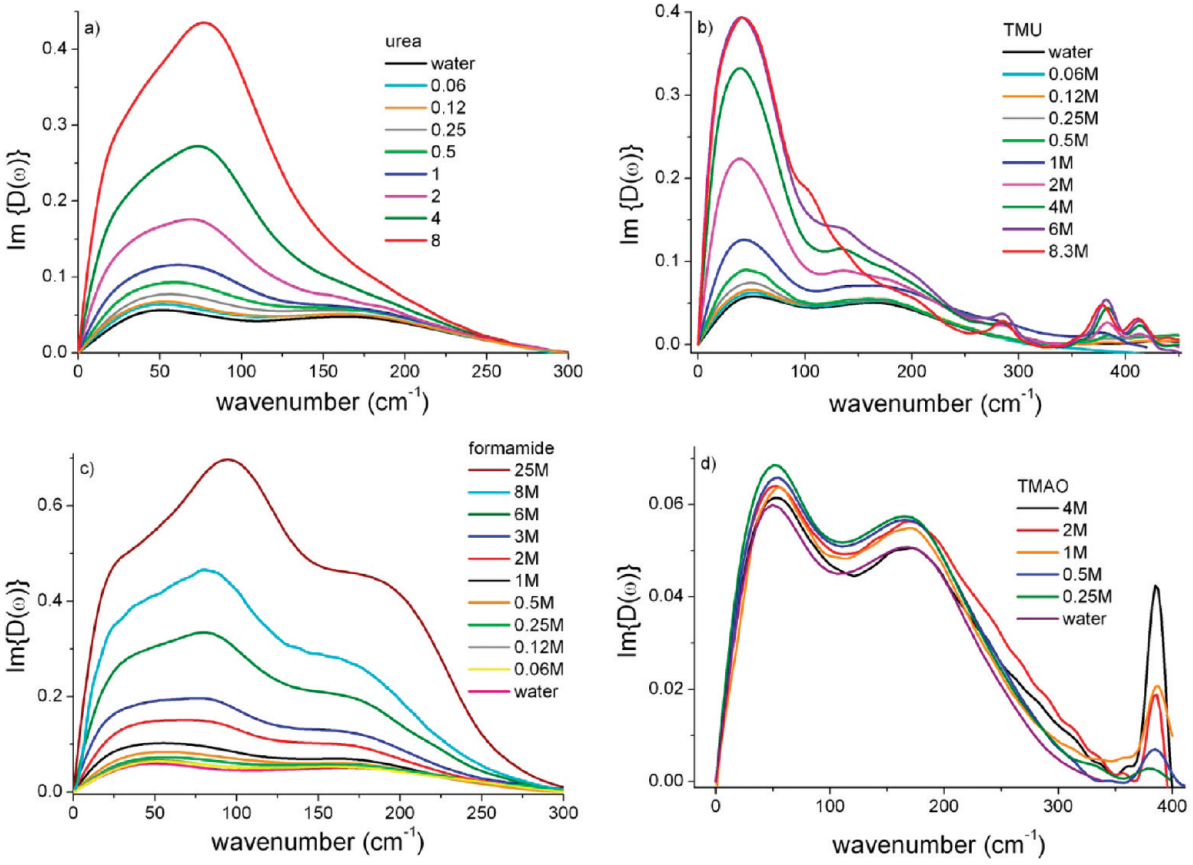

Figure 5. Im $D'(\omega)$ for UA, FA, TMAO, and TMU as a function of concentration. The Raman spectral density of pure water (black) is plotted as a reference.

contribution of TMU to the OKE signal suggests that a fraction of the nuclear OKE response may arise from the solute, even at concentrations below 1 M. This observation correlates with the requirement for a third relaxation time in the picosecond dynamics, which was proposed above to have its origin in solute molecular reorientation.

The Im $D'(\omega)$ measured for solute concentrations between 0 and 0.5 M are very similar to one another. At these low concentrations, they retain the bimodal shape characteristic of liquid water. Thus, we conclude that the structure of liquid water is maintained at these low solute concentrations, even though the collective picosecond time scale relaxation dynamics are slowed appreciably by the presence of the solute, as described above. At concentrations exceeding 0.5 M, there is a considerable divergence in the shape of the spectral densities. For TMAO, the Im $D'(\omega)$ are remarkably independent of solute concentration, apart from the appearance of a mode at $\sim$380 cm^{-1} which increases in amplitude linearly with increasing solute concentration (Figure 5d). This mode is assigned to an intramolecular Raman active vibration. For UA and FA, the increased amplitude in Im $D'(\omega)$ with increasing concentration above 0.5 M is accompanied by the growth of a band around 100 cm^{-1} which is absent in pure water. For TMU above 0.5 M, the amplitude also increases sharply and is dominated by strong growth in the band at low frequency, which is also evident in neat TMU. The Raman spectrum of TMU was investigated through DFT, and two components were found in this low frequency regime ($\sim$55 and $\sim$130 cm^{-1}) as well as modes at higher frequency, 285, 378, and 412 cm^{-1} (also evident in Figure 5b). More details of the DFT calculations are presented in the Supporting Information. On the basis of these, we tentatively assign the additional component in the Im $D'(\omega)$ of TMU to molecular modes of the solute.

The spectral densities were analyzed quantitatively as follows. The Im $D'(\omega)$ of TMAO were fit with two line shape functions, the Bucaro−Litovitz (BL) and an antisymmetrized Gaussian (ASG). The BL[68] function

$$I_{BL} = A_{BL}\omega^{\alpha} \exp[-(\omega/\omega_{BL})] \quad (8)$$

fits the lowest frequency component, $\sim$45 cm^{-1}, where the fitting parameters are the amplitude, A_{BL}, a characteristic frequency, ω_{BL}, and the exponent α. The highest frequency component at $\sim$175 cm^{-1} is represented by the ASG:

$$I_{ASG} = A_{ASG}\left[\exp\left[-\frac{\omega-\omega_{ASG}}{\Delta\omega_{ASG}}\right]^2 - \exp\left[-\frac{\omega+\omega_{ASG}}{\Delta\omega_{ASG}}\right]^2\right] \quad (9)$$

where A_{ASG} is the amplitude, ω_{ASG} is the central frequency, and $\Delta\omega_{ASG}$ is the full width at half-maximum.

The same two functions also adequately fit the Im $D'(\omega)$ of pure water, where they have been assigned to H-bond stretching and bending modes (see above). At concentrations below 0.5 M, the UA and FA spectral densities were also all fit solely with these two functions. Thus, this analysis procedure permits quantification of the evolution of the THz spectral densities of UA, FA, and TMAO solutions as a function of solute concentration. A third

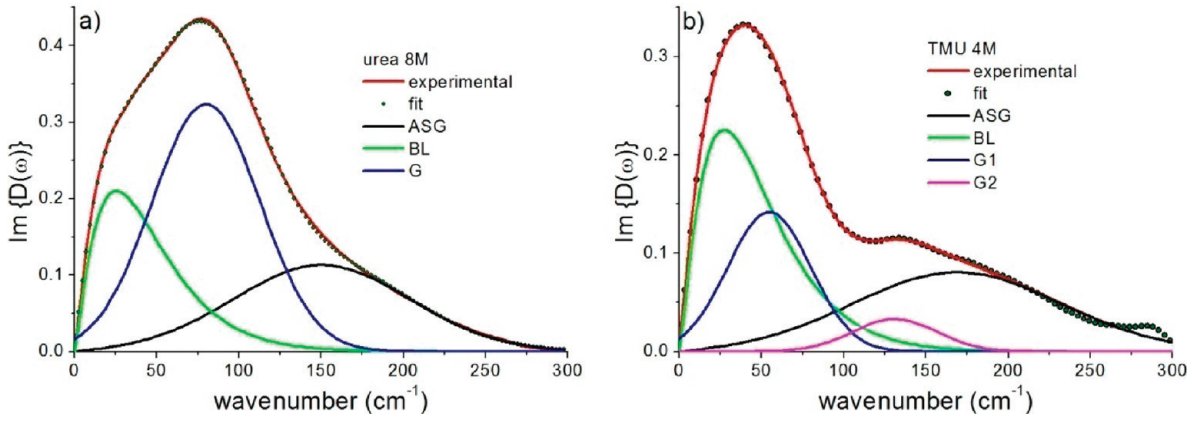

Figure 6. (a) Im $D'(\omega)$ of 8 M UA fitted with three functions. BL, G, and ASG denote Bucaro−Litovitz, Gaussian, and antisymmetrized Gaussian, respectively. The red line is experimental data and green dots are the sum of the three fitting functions. (b) The same as part a except for TMU, including additional Gaussian components.

function, a Gaussian (G), was required to fit the spectral densities of UA and FA at concentrations above 0.5 M given by

$$I_G = A_G \exp\left[-\frac{\omega - \omega_G}{\Delta\omega_G}\right]^2 \qquad (10)$$

where A_G is the amplitude, ω_G is the center frequency, and $\Delta\omega_G$ is the full width at half-maximum. Numerical values obtained from this fitting procedure, which gave good quality fits for these three solutes (e.g., Figure 6a), are presented in the Supporting Information. The spectra for solutions of TMU above 1 M were more complex and below 250 cm^{-1} could only be successfully reproduced by a sum of BL, ASG, and two Gaussians at 55 and 135 cm^{-1}, which are proposed to reflect the intramolecular solute modes found in the DFT calculation (see above); the fit is shown in Figure 6b. Frequencies and amplitudes obtained from the fit to all spectral densities are plotted in Figure 7. The two low frequency Gaussian components for TMU are omitted for clarity.

For TMAO, the amplitudes and frequencies of both BL and ASG functions in the whole range of concentration are constant and, within experimental error, the same as those for pure water. This result indicates that the water structure, as indicated by the characteristic bimodal Im $D'(\omega)$, is remarkably well preserved in the TMAO solutions, even at 4 M concentration. This is consistent with some molecular dynamics simulations[18] where it was found that the water hydrogen-bond network is little affected by the presence of a hydrophobic solute. The same conclusion was reached through the analysis of neutron scattering[69] data for methane−water solutions. The retention of this structure even at 4 M is however surprising and may suggest microscopic clustering of the TMAO solute to leave larger volumes of contiguous bulk-like water. In contrast to the THz spectral density, the mid-IR absorption spectra of increasingly concentrated TMAO solutions were reported to reveal a red shift of the OH stretching mode.[70] Two explanations were suggested. First that there is a strengthening of water−water H-bonds in the vicinity of a hydrophobic TMAO methyl group[70] and second that the red shift is caused by an increasing fraction of strong H-bonds with the hydrophilic oxygen in TMAO.[16] In either case, the present data suggest that the underlying tetrahedral water structure is not highly perturbed by the water−TMAO interaction.

The Im $D'(\omega)$ for FA and UA are composed of three modes, the BL, ASG, and, at high concentrations only, an intermediate frequency G mode. The low frequency Raman spectra of aqueous solutions of FA and UA have been discussed elsewhere.[4,63,71,72] However, the concentrations studied were typically higher than those considered here. At concentrations below 0.5 M, the Im $D'(\omega)$ of UA and FA are characterized completely by the two modes characteristic of pure water at ∼45 and 175 cm^{-1} (Figure 7). The frequencies of both the BL and ASG modes are constant below 1 M but shift slightly to the red above this concentration, the biggest shift being observed for UA. The red shift of the ASG is accompanied by an increasing amplitude, which is much more marked for FA than UA. The decrease in frequency of the ASG is assigned to the disruption or distortion of the tetrahedral structure in liquid water. This in turn indicates a perturbation to water−water hydrogen bonds by the solute. It is significant that at these high concentrations (>1 M) almost all water molecules will be found in the hydration shell of a solute, so it is apparently only under conditions of such high solute concentration that the water−water H-bond structure is significantly disrupted. The increase in amplitude of the ASG is more difficult to assign but may suggest a larger Raman cross section for water−UA/FA modes than for water−water modes, although for the highest FA concentrations a molecular component may become significant (see below).

As the concentration increases further, the contribution of the solute orientational (librational) dynamics is expected to become more significant. Molecular dynamics simulations coupled to the calculation of polarizability anisotropy relaxation[64] suggest that above a mole fraction of 0.05 FA in water (i.e., a 2.5 M solution) the FA libration, modified by its interaction with water, begins to make a contribution to the OKE signal, which increases further with additional FA. In line with this assignment, the decrease in frequency of the ASG mode for FA continues only until a concentration of 6 M (Figure 7), above which it begins to increase, eventually reaching ∼184 cm^{-1} for pure FA (25 M, data not shown); this mode in pure FA has previously been assigned to a molecular libration.[63,72]

The G mode required to fit the Im $D'(\omega)$ spectra of FA and UA grows in importance at concentrations above 0.5 M. Its amplitude increases linearly with concentration, suggesting that it is associated with the solute. The frequency of the mode also increases with increasing concentration, suggesting the formation of stronger hydrogen bonded structures in the solution when fewer water molecules are available for solvation. Idrissi also resolved the low frequency Raman spectra for UA in water

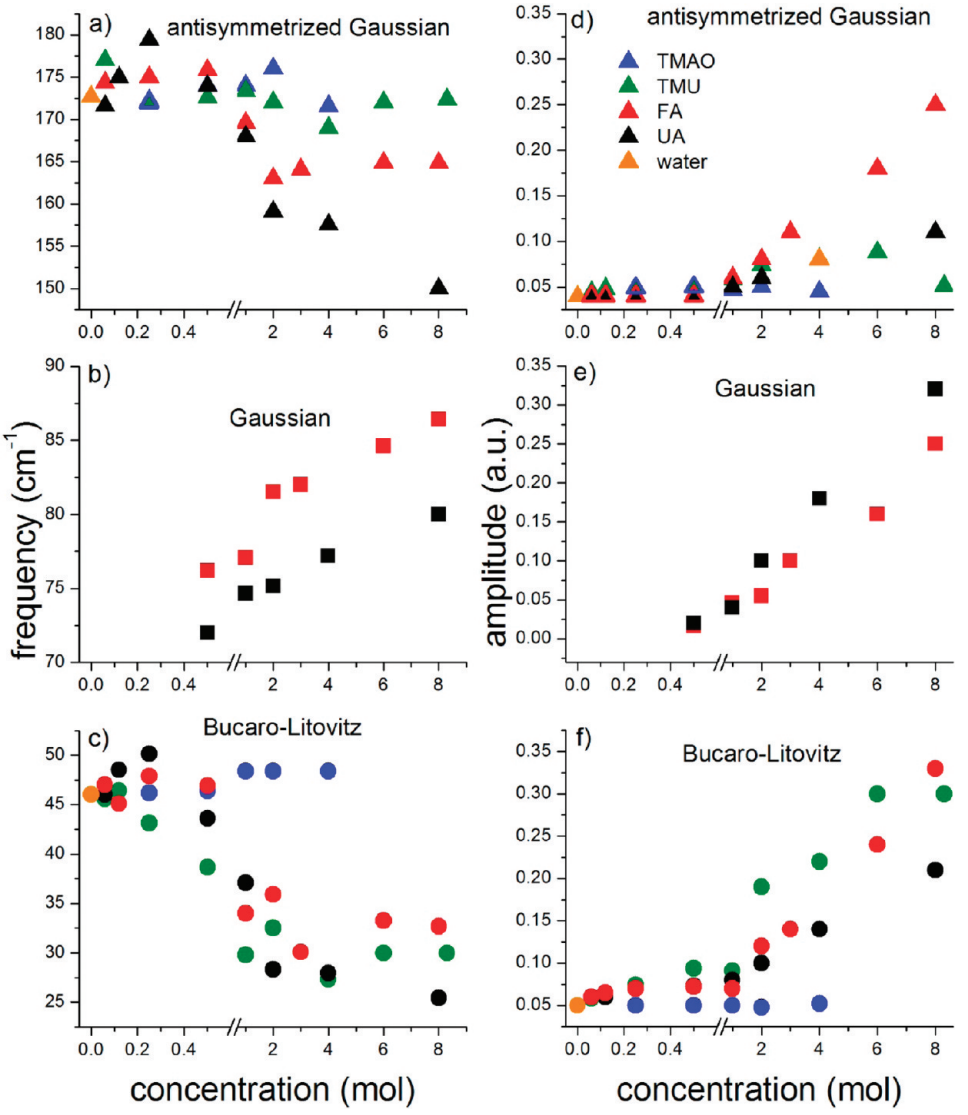

Figure 7. Frequency and amplitudes of fitted spectral components for all four solutes studied. Gaussian is the intermediate component observed for UA and FA, which is not required to fit the data below 0.5 M.

into three components.[71] In that work, a red shift of the ASG was recovered, as seen here, but the low frequency component was reported to show an increase in frequency with increasing concentration while a constant frequency for the intermediate Gaussian mode was recovered. These small differences may arise because of the different fitting functions used and because the spectra measured in the frequency domain below 50 cm^{-1} may not be as well resolved as in the OKE measurement (due to the thermal occupation factor).[71]

To investigate the origin of this solute mode, DFT calculations were performed for UA and UA plus specific waters. A new low frequency Raman active out-of-plane bending mode appears at 73 cm^{-1} for the UA water complex. This suggests an assignment of G to a water−UA mode, consistent with the linear concentration dependence. However, a similar mode appeared for DFT calculations on UA dimers, yielding a 99 cm^{-1} mode with larger amplitude than the water−UA mode, suggesting an alternative assignment of G to a UA dimer mode. Additional calculations on a UA dimer structure linked by two intervening water molecules also showed a band in the correct location for G. DFT calculations on the FA water complex also predict a mode near 100 cm^{-1} but with very small amplitude. In contrast, calculations on the FA dimer predict an intense mode of the correct frequency, favoring a dimer assignment for G in FA solutions. The key feature in all of these calculations is that this mode only arises in the presence of hydrogen bonding to the solute, and is not found in the isolated molecule. Nielsen at al.[73] studied low frequency spectra of *N*-methylformamide and dimethylformamide and found a 90 cm^{-1} mode in the former but not the latter. He concluded that this mode is only present in amides capable of forming hydrogen bonds. Castner et al.[63] studied the same solutes using OHD−OKE and reached the same conclusion. On the basis of the DFT calculations and these earlier studies, we assign the G mode observed for FA and UA solutions to out-of-plane bending of an H-bonded solute complex, which may include both solute−solute and solute−water complexes, or a more extended network.

The Im $D'(\omega)$ spectra of TMU at concentrations below 0.5 M are similar to those for pure water (as for the other solutes). Above this concentration, a number of new modes appear, which

dx.doi.org/10.1021/jp111764p |*J. Phys. Chem. B* 2011, 115, 2563–2573

serve to complicate the assignment. This is consistent with the relatively large contribution of the TMU solute to the Im $D'(\omega)$. An example of the multicomponent fit to the Im $D'(\omega)$ of TMU is shown in Figure 6b. From the point of view of comparing these results with those for other solutes, a useful result from Figure 6b is that the contributions of the BL and ASG modes can still be followed as a function of concentration. The BL band shifts to the lower frequency with increasing concentration and increases in amplitude. The same result was found in the case of FA, but it is difficult to separate the solute contribution from the water contribution to these spectra. However, the ~175 cm^{-1} ASG mode, taken to be characteristic of the tetrahedral water structure, remains unchanged over the whole range of concentration (Figure 7). The absence of a shift in this ASG mode suggests that the H-bonded water structure in the TMU−water solutions is similar to that of bulk water, as was also observed for TMAO solutions. Thus, although the TMU assignment is less certain because of the complexity of the spectrum, the data are consistent with a weak perturbation to the water structure by this hydrophobic solute.

CONCLUSION

The ultrafast OHD−OKE experiment has been used to probe the dynamics of a series of aqueous solutions. Two hydrophobic and two hydrophilic solutes were investigated over concentration ranges from <0.1 M to saturated solutions or neat liquid. The OHD−OKE reports simultaneously the THz Raman spectral density of the solution and the collective picosecond relaxation dynamics of its H-bonded network. Two distinct concentration regimes were identified. At low concentration (<0.5 M), the THz spectrum is similar to that of pure water, showing that the water structure is largely retained. Picosecond relaxation in the H-bonded network measured under these conditions was analyzed as a weighted sum of bulk-like and solvation water relaxation. Solvation water exhibited slower relaxation than the bulk in all cases. The effect was modest for hydrophobic solutes (a factor of 2−3). There was no evidence for immobilization of water by hydrophobic solutes.[5] The effect of hydrophilic solutes on relaxation within the H-bonded network was about a factor of 2 larger than that for hydrophobic solutes. This result is consistent with simulations of the reorientation of water molecules in the solvation shell.[16]

As the concentration increases above 1 M, the slowest component in the picosecond dynamics begins to dominate, consistent with an appreciable slow-down in the relaxation mechanism when the majority of water molecules are involved in a solute's solvation shell. In hydrophilic solutes, this slow down correlates with disruption of the water structure in the THz Raman spectral density, specifically a red shift of the ca. 175 cm^{-1} component observed in the pure water spectrum and assigned to H-bond stretching in a tetrahedral geometry. This suggests that the slowest dynamics at high solute concentration are associated with a disrupted water structure. The correlation observed here between a slow-down in relaxation dynamics and disruption of the local water structure suggests that the slow (>10 ps) dynamics which have been reported to dominate water orientational relaxation at higher solute concentrations may more properly be associated with confined rather than interfacial water.

The surprisingly weak perturbation to the spectral density by the hydrophobic TMAO solute is consistent with the hydrophobic solute having a minimal effect on the water structure. That this weak perturbation is maintained up to 4 M is suggestive of solute clustering in this solution. As the solute concentration increases, the Raman spectral densities for FA, UA, and TMU come to be dominated by the solute contribution. This is particularly marked for TMU, where low frequency molecular modes contribute at all frequencies. For the hydrophilic solutes UA and FA, the changes in the water spectral density are accompanied by the growth of a new mode associated with an H-bonded solute.

ASSOCIATED CONTENT

Supporting Information. The longer time OKE response and details of DFT calculations and fitting parameters in the time and frequency domain. This material is available free of charge via the Internet at http://pubs.acs.org.

AUTHOR INFORMATION

Corresponding Author
*E-mail: s.meech@uea.ac.uk.

ACKNOWLEDGMENT

We are grateful to EPSRC for financial support (EP/E010466/1), and K.M. thanks UEA for the award of a studentship.

REFERENCES

(1) Bakulin, A. A.; Liang, C.; Jansen, T. L.; Wiersma, D. A.; Bakker, H. J.; Pshenichnikov, M. S. *Acc. Chem. Res.* **2009**, *42*, 1229.
(2) Grdadolnik, J.; Marechal, Y. *J. Mol. Struct.* **2002**, *615*, 177.
(3) Hernandezcobos, J.; Ortegablake, I.; Bonillamarin, M.; Morenobello, M. *J. Chem. Phys.* **1993**, *99*, 9122.
(4) Idrissi, A.; Bartolini, P.; Ricci, M.; Righini, R. *J. Chem. Phys.* **2001**, *114*, 6774.
(5) Rezus, Y. L. A.; Bakker, H. J. *Phys. Rev. Lett.* **2007**, *99*, 148301.
(6) Rezus, Y. L. A.; Bakker, H. J. *J. Phys. Chem. A* **2008**, *112*, 2355.
(7) Halle, B. *Philos. Trans. R. Soc., B* **2004**, *359*, 1207.
(8) Johnson, M. E.; Malardier-Jugroot, C.; Murarka, R. K.; Head-Gordon, T. *J. Phys. Chem. B* **2009**, *113*, 4082.
(9) Russo, D.; Hura, G.; Head-Gordon, T. *Biophys. J.* **2004**, *86*, 1852.
(10) Russo, D.; Murarka, R. K.; Copley, J. R. D.; Head-Gordon, T. *J. Phys. Chem. B* **2005**, *109*, 12966.
(11) Ball, P. *Chem. Rev.* **2008**, *108*, 74.
(12) Helms, V. *ChemPhysChem* **2007**, *8*, 23.
(13) Papoian, G. A.; Ulander, J.; Eastwood, M. P.; Luthey-Schulten, Z.; Wolynes, P. G. *Proc. Natl. Acad. Sci. U.S.A.* **2004**, *101*, 3352.
(14) Laage, D.; Stirnemann, G.; Hynes, J. T. *J. Phys. Chem. B* **2009**, *113*, 2428.
(15) Qvist, J.; Halle, B. *J. Am. Chem. Soc.* **2008**, *130*, 10345.
(16) Stirnemann, G.; Hynes, J. T.; Laage, D. *J. Phys. Chem. B* **2010**, *114*, 3052.
(17) Colombo, M. F.; Rau, D. C.; Parsegian, V. A. *Science* **1992**, *256*, 655.
(18) Kuffel, A.; Zielkiewicz, J. *J. Chem. Phys.* **2010**, 133.
(19) Belletato, P.; Freitas, L. C. G.; Areas, E. P. G.; Santos, P. S. *Phys. Chem. Chem. Phys.* **1999**, *1*, 4769.
(20) Zhao, H. *Biophys. Chem.* **2006**, *122*, 157.
(21) Wei, H. Y.; Fan, Y. B.; Gao, Y. Q. *J. Phys. Chem. B* **2010**, *114*, 557.
(22) Szekely, N. K.; Almasy, L.; Jancso, G. *J. Mol. Liq.* **2007**, *136*, 184.
(23) Walrafen, G. E. *J. Chem. Phys.* **1966**, *44*, 3726.
(24) Hammes, G. G.; Schimmel, P. R. *J. Am. Chem. Soc.* **1967**, *89*, 442.
(25) Hayashi, Y.; Katsumoto, Y.; Omori, S.; Kishii, N.; Yasuda, A. *J. Phys. Chem. B* **2007**, *111*, 1076.

(26) Chitra, R.; Smith, P. E. *J. Phys. Chem. B* **2000**, *104*, 5854.
(27) Stumpe, M. C.; Grubmuller, H. *J. Phys. Chem. B* **2007**, *111*, 6220.
(28) Sacco, A.; Holz, M. *J. Chem. Soc., Faraday Trans.* **1997**, *93*, 1101.
(29) Subraman, S; Balasubr, D; Ahluwali., Jc. *J. Phys. Chem.* **1969**, *73*, 266.
(30) Jerie, K.; Baranowski, A.; Glinski, J.; Orzechowski, K. *J. Phys. IV* **1993**, *3*, 135.
(31) Frank, H. S.; Evans, M. W. *J. Chem. Phys.* **1945**, *13*, 507.
(32) Hoccart, X.; Turrell, G. *J. Chem. Phys.* **1993**, *99*, 8498.
(33) Soper, A. K.; Castner, E. W.; Luzar, A. *Biophys. Chem.* **2003**, *105*, 649.
(34) Idrissi, A.; Gerard, M.; Damay, P.; Kiselev, M.; Puhovsky, Y.; Cinar, E.; Lagant, P.; Vergoten, G. *J. Phys. Chem. B* **2010**, *114*, 4731.
(35) Tovchigrechko, A.; Rodnikova, M.; Barthel, J. *J. Mol. Liq.* **1999**, *79*, 187.
(36) Shimizu, A.; Fumino, K.; Yukiyasu, K.; Taniguchi, Y. *J. Mol. Liq.* **2000**, *85*, 269.
(37) Castner, E. W.; Chang, Y. J.; Chu, Y. C.; Walrafen, G. E. *J. Chem. Phys.* **1995**, *102*, 653.
(38) Torre, R.; Bartolini, P.; Righini, R. *Nature* **2004**, *428*, 296.
(39) Saito, S.; Ohmine, I. *J. Chem. Phys.* **1997**, *106*, 4889.
(40) Mazur, K.; Heisler, I. A.; Meech, S. R. *J. Phys. Chem. B* **2010**, *114*, 10684.
(41) Smith, N. A.; Meech, S. R. *Int. Rev. Phys. Chem.* **2002**, *21*, 75.
(42) Hunt, N. T.; Jaye, A. A.; Meech, S. R. *Phys. Chem. Chem. Phys.* **2007**, *9*, 2167.
(43) Zhong, Q.; Fourkas, J. T. *J. Phys. Chem. B* **2008**, *112*, 15529.
(44) Hunt, N. T.; Jaye, A. A.; Hellman, A.; Meech, S. R. *J. Phys. Chem. B* **2004**, *108*, 100.
(45) McMorrow, D.; Lotshaw, W. T.; Kenneywallace, G. A. *IEEE J. Quantum Electron.* **1988**, *24*, 443.
(46) Lotshaw, W. T.; McMorrow, D.; Thantu, N.; Melinger, J. S.; Kitchenham, R. *J. Raman Spectrosc.* **1995**, *26*, 571.
(47) Watanabe, J.; Tohji, M.; Ohtsuka, E.; Miyake, Y.; Kinoshita, S. *Chem. Phys. Lett.* **2004**, *396*, 232.
(48) *Handbook of Chemistry and Physics*, 85th ed.; CRC Press: Boca Raton, Florida, 2004.
(49) Okpala, C.; Guiseppielie, A.; Maharajh, D. M. *J. Chem. Eng. Data* **1980**, *25*, 384.
(50) Sinibaldi, R.; Casieri, C.; Melchionna, S.; Onori, G.; Segre, A. L.; Viel, S.; Mannina, L.; De Luca, F. *J. Phys. Chem. B* **2006**, *110*, 8885.
(51) Taniewskaosinska, S.; Piekarska, A.; Kacperska, A. *J. Solution Chem.* **1983**, *12*, 717.
(52) Frisch, M. J.; Trucks, G. W.; Schlegel, H. B.; Scuseria, G. E.; Robb, M. A.; Cheeseman, J. R.; Montgomery, J. A., Jr.; Vreven, T.; Kudin, K. N.; Burant, J. C.; Millam, J. M.; Iyengar, S. S.; Tomasi, J.; Barone, V.; Mennucci, B.; Cossi, M.; Scalmani, G.; Rega, N.; Petersson, G. A.; Nakatsuji, H.; Hada, M.; Ehara, M.; Toyota, K.; Fukuda, R.; Hasegawa, J.; Ishida, M.; Nakajima, T.; Honda, Y.; Kitao, O.; Nakai, H.; Klene, M.; Li, X.; Knox, J. E.; Hratchian, H. P.; Cross, J. B.; Bakken, V.; Adamo, C.; Jaramillo, J.; Gomperts, R.; Stratmann, R. E.; Yazyev, O.; Austin, A. J.; Cammi, R.; Pomelli, C.; Ochterski, J. W.; Ayala, P. Y.; Morokuma, K.; Voth, G. A.; Salvador, P.; Dannenberg, J. J.; Zakrzewski, V. G.; Dapprich, S.; Daniels, A. D.; Strain, M. C.; Farkas, O.; Malick, D. K.; Rabuck, A. D.; Raghavachari, K.; Foresman, J. B.; Ortiz, J. V.; Cui, Q.; Baboul, A. G.; Clifford, S.; Cioslowski, J.; Stefanov, B. B.; Liu, G.; Liashenko, A.; Piskorz, P.; Komaromi, I.; Martin, R. L.; Fox, D. J.; Keith, T.; Al-Laham, M. A.; Peng, C. Y.; Nanayakkara, A.; Challacombe, M.; Gill, P. M. W.; Johnson, B.; Chen, W.; Wong, M. W.; Gonzalez, C.; Pople, J. A. *Gaussian 03*; Gaussian, Inc.: Wallingford, CT, 2004.
(53) Palese, S.; Schilling, L.; Miller, R. J. D.; Staver, P. R.; Lotshaw, W. T. *J. Phys. Chem.* **1994**, *98*, 6308.
(54) Winkler, K.; Lindner, J.; Bursing, H.; Vohringer, P. *J. Chem. Phys.* **2000**, *113*, 4674.
(55) Winkler, K.; Lindner, J.; Vohringer, P. *Phys. Chem. Chem. Phys.* **2002**, *4*, 2144.
(56) Walrafen, G. E.; Chu, Y. C.; Piermarini, G. J. *J. Chem. Phys.* **1996**, *100*, 10363.
(57) Ohmine, I.; Saito, S. *Acc. Chem. Res.* **1999**, *32*, 741.
(58) Mazzacurati, V.; Nucara, A.; Ricci, M. A.; Ruocco, G.; Signorelli, G. *J. Chem. Phys.* **1990**, *93*, 7767.
(59) Ohmine, I.; Tanaka, H. *Chem. Rev.* **1993**, *93*, 2545.
(60) Marti, J.; Padro, J. A.; Guardia, E. *J. Chem. Phys.* **1996**, *105*, 639.
(61) Murphy, W. F. *J. Chem. Phys.* **1977**, *67*, 5877.
(62) Sonoda, M. T.; Vechi, S. M.; Skaf, M. S. *Phys. Chem. Chem. Phys.* **2005**, *7*, 1176.
(63) Chang, Y. J.; Castner, E. W. *J. Chem. Phys.* **1993**, *99*, 113.
(64) Elola, M. D.; Ladanyi, B. M. *J. Chem. Phys.* **2007**, 126.
(65) Paolantoni, M.; Sassi, P.; Morresi, A.; Santini, S. *J. Chem. Phys.* **2007**, 127.
(66) Lee, S. L.; Debenedetti, P. G.; Errington, J. R. *J. Chem. Phys.* **2005**, 122.
(67) Tielrooij, K. J.; Hunger, J.; Buchner, R.; Bonn, M.; Bakker, H. J. *J. Am. Chem. Soc.* **2010**, *132*, 15671.
(68) Bucaro, J. A.; Litovitz, T. A. *J. Chem. Phys.* **1971**, *54*, 3846.
(69) Buchanan, P.; Aldiwan, N.; Soper, A. K.; Creek, J. L.; Koh, C. A. *Chem. Phys. Lett.* **2005**, *415*, 89.
(70) Sharp, K. A.; Madan, B.; Manas, E.; Vanderkooi, J. M. *J. Chem. Phys.* **2001**, *114*, 1791.
(71) Idrissi, A. *Spectrochim. Acta, Part A* **2005**, *61*, 1.
(72) Chang, Y. J.; Castner, E. W. *J. Phys. Chem.* **1994**, *98*, 9712.
(73) Colaianni, S. E. M.; Nielsen, O. F. *J. Mol. Struct.* **1995**, *347*, 267.